

Correcting North Atlantic sea surface salinity biases in the Kiel Climate Model: influences on ocean circulation and Atlantic Multidecadal Variability

T. Park¹ · W. Park¹ · M. Latif^{1,2}

Received: 17 August 2015 / Accepted: 4 January 2016 / Published online: 20 January 2016
© Springer-Verlag Berlin Heidelberg 2016

Abstract A long-standing problem in climate models is the large sea surface salinity (SSS) biases in the North Atlantic. In this study, we describe the influences of correcting these SSS biases on the circulation of the North Atlantic as well as on North Atlantic sector mean climate and decadal to multidecadal variability. We performed integrations of the Kiel Climate Model (KCM) with and without applying a freshwater flux correction over the North Atlantic. The quality of simulating the mean circulation of the North Atlantic Ocean, North Atlantic sector mean climate and decadal variability is greatly enhanced in the freshwater flux-corrected integration which, by definition, depicts relatively small North Atlantic SSS biases. In particular, a large reduction in the North Atlantic cold sea surface temperature bias is observed and a more realistic Atlantic Multidecadal Variability simulated. Improvements relative to the non-flux corrected integration also comprise a more realistic representation of deep convection sites, sea ice, gyre circulation and Atlantic Meridional Overturning Circulation. The results suggest that simulations of North Atlantic sector mean climate and decadal variability could strongly benefit from alleviating sea surface salinity biases in the North Atlantic, which may enhance the skill of decadal predictions in that region.

Keywords Sea surface salinity · Climate modeling · Model bias · Atlantic meridional overturning circulation · Atlantic multidecadal variability

1 Introduction

Most models which participated in the Coupled Model Intercomparison Project Phase 5 (CMIP5, Taylor et al. 2012) and that were discussed in the Intergovernmental Panel on Climate Change (IPCC) Fifth Assessment Report (AR5) have deficiencies and biases that introduce large uncertainties in their products (Flato et al. 2013). Wang et al. (2014) show that biases in special regions can be linked with biases that are globally remote. In particular, they find that sea surface temperature (SST) biases in the North Atlantic are commonly linked with the Atlantic Meridional Overturning Circulation (AMOC), a current system which is characterized by the northward flow of warm waters in the upper ocean and returning southward flow of cold waters in the deep ocean. A weak AMOC, for example, is not only associated with cold North Atlantic SST but also with cold surface air temperature (SAT) biases in the entire Northern Hemisphere and an atmospheric circulation bias pattern that resembles the Northern Hemisphere annular mode (NAM; e.g., Thompson and Wallace 1998). Moreover, a weak AMOC results in warm Southern Hemisphere SAT biases (Wang et al. 2014).

Attempts to alleviate the SST biases in the North Atlantic have generally not been successful during the past decade (Flato et al. 2013). Too coarse model resolution may be one reason for this failure, but high-resolution climate models often depict biases similar to those seen in their coarse-resolution counterparts (e.g., Delworth et al. 2012). Another suspect for causing the large SST biases is North

Electronic supplementary material The online version of this article (doi:10.1007/s00382-016-2982-1) contains supplementary material, which is available to authorized users.

✉ M. Latif
mlatif@geomar.de

¹ GEOMAR Helmholtz-Zentrum für Ozeanforschung Kiel, Kiel, Germany

² Universität Kiel, Kiel, Germany

Atlantic upper ocean salinity. In fact, the simulation of sea surface salinity (SSS) in that region is relatively poor in many climate models (Flato et al. 2013). For example, values of SSS in the subpolar North Atlantic and the Arctic tend to be too low. This increases stratification, which hampers convection and as a consequence, many climate models possess excessive sea ice and also misplace deep convection sites. For example, deep convection is often found south of Greenland and not in the Labrador Sea which measurements indicate as an important source region of the North Atlantic Deep Water (NADW) (Marshall and Schott 1999). Further, the fresh SSS bias has the potential to weaken the AMOC through lowering the density in the high-latitude sinking regions. It is well known that there is a positive feedback between the AMOC-strength and upper-ocean salinity in the mid- and high-latitude North Atlantic: a stronger (weaker) AMOC transports more (less) salt from the subtropics to the north, enhancing (reducing) upper-ocean density in the sinking regions, which in turn tends to further strengthen (weaken) the AMOC through enhanced deep convection (e.g.; Hofmann and Rahmstorf 2009). This positive feedback could be one reason for the large sensitivity of climate models to errors in either of their individual model components: the atmosphere, ocean and sea ice. All three subsystems strongly interact with each other in the North Atlantic region, which has the potential to amplify SSS biases originating in either of the individual model components.

The North Atlantic is a region of strong decadal to multidecadal variability. For example, instrumental measurements across the North Atlantic and proxy data suggest multidecadal swings in SST (Delworth and Mann 2000; Latif et al. 2004; Knight et al. 2005; Gulev et al. 2013), a phenomenon which is referred to as the Atlantic Multidecadal Variability (AMV) or Atlantic Multidecadal Oscillation (AMO). In the following, we shall use the term AMV throughout the paper. Most climate models suggest that the AMV, at least in part, is forced by variations of the AMOC (Ba et al. 2014): a positive AMV-phase corresponds to an anomalously strong AMOC and vice versa. Wang and Zhang (2013) show that in climate models, multidecadal upper ocean temperature and salinity variability in the tropical North Atlantic involves the AMV, AMOC and subtropical cell (STC). High-latitude SSS biases, through their impact on the AMOC, may therefore also lead to biases in tropical Atlantic sector climate variability.

Climate models depict a large spread in the overall representation of the AMV (spatial pattern, periodicity and amplitude), in the relationships between different variables relevant to the AMV and nature of atmosphere–ocean–sea ice interactions in the North Atlantic region (Ba et al. 2014). For example, the link between the AMOC and the AMV widely differs among climate models. Large spread

also is observed with regard to the forcing of the AMOC by the North Atlantic Oscillation (NAO, Hurrell 1995) which is the leading mode of North Atlantic sector atmospheric variability in winter. Even the sign of this relationship can differ from model to model (Ba et al. 2014). Latif et al. (2006), by analyzing observations and model results, found some support for the conjecture that the low-frequency portion of the NAO-related heat flux variability, by impacting Labrador Sea deep convection, forces multidecadal AMOC variability which in turn drives the AMV. Such a link between the NAO and the AMOC, however, is absent in a number of climate models. Is it possible that the North Atlantic SSS biases not only influence SST and SAT but also the NAO/AMOC relationship and thus the character of the decadal to multidecadal variability in the North Atlantic sector? And if so, what is the physics behind this influence? This is the topic of this paper.

We use the Kiel Climate Model (KCM; Park et al. 2009) to address these questions. Salinity plays an important role in the AMOC variability and AMV simulated in a previous version of the KCM (Ba et al. 2013): wintertime convection in the Irminger Sea, which drives the AMV, is mainly controlled by salinity anomalies transported by the subpolar gyre into this region. We investigate the influence of North Atlantic SSS biases in a version of the KCM employing an atmosphere model with a higher horizontal resolution. This is done by removing most of the North Atlantic SSS biases by means of a freshwater flux correction and by comparing the results with those of a control run without that correction. The paper is organized as follows: Sect. 2 briefly describes the KCM version used here, the methodology used to compute the flux correction, the experimental setup and the observations used in this study. In Sect. 3, we provide the comparison of the two integrations which differ only in the application of a freshwater flux correction in the North Atlantic. The major findings are summarized and discussed in Sect. 4.

2 Model, freshwater flux correction and experimental design, and observations

The version of the Kiel Climate Model used here consists of the ECHAM5 atmosphere general circulation model with a spectral horizontal resolution of T42 ($2.8^\circ \times 2.8^\circ$) and with 19 vertical levels. The atmosphere model is coupled through the OASIS coupler to the NEMO ocean–sea ice model integrated on the global tripolar grid at 2° horizontal resolution (ORCA2). Enhanced meridional resolution of 0.5° is employed in the equatorial region, and the ocean model is run with 31 levels. We note that the standard KCM (Park et al. 2009), which was used in e.g., Ba et al. (2013, 2014), employs a coarser horizontal resolution of T31

($3.75^\circ \times 3.75^\circ$) in its atmospheric component. A list of references of published studies conducted with the standard KCM can be obtained from <http://www.geomar.de/en/research/fb1/fb1-me/research-topics/climate-modelling/kcms/>.

The KCM suffers from significant biases in the North Atlantic which, as mentioned above, are common to many climate models. The aforementioned SSS biases in the high latitudes are one example. Another example is the rather strong North Atlantic cold SST bias amounting to several centigrade. This bias largely originates from a too zonal path of the North Atlantic Current, i.e. the missing Northwest Corner, and also from a too weak AMOC (Drews et al. 2015). Here we investigate the impact of correcting the North Atlantic SSS biases on the ocean circulation of the North Atlantic and North Atlantic sector decadal to multidecadal climate variability. This is achieved by artificially removing most of the SSS biases from the KCM by means of a freshwater flux correction (Manabe and Stouffer 1988; Sausen et al. 1988) that is only applied over the North Atlantic.

The experimental strategy is as follows: We perform three experiments. The first experiment is a 2000 year long pre-industrial control run employing a CO_2 -concentration of 286 ppm and starting from Levitus climatology. In the second experiment, initial conditions are again from Levitus climatology but the SSSs in the North Atlantic (10°N – 80°N) are restored to monthly SSSs from Levitus climatology with a relaxation timescale of 30 days. In this run, present-day CO_2 -concentration of 348 ppm is used in order to be consistent with the Levitus surface forcing. This restoring-experiment has a length of 100 years. The resulting monthly surface freshwater fluxes were diagnosed from the last 50 years of the restoring-experiment (Fig. 1), when the area-averaged North Atlantic SSS has basically equilibrated. In the third experiment, these freshwater fluxes are then added to the model during a 1000-yr long integration employing pre-industrial CO_2 -concentration and initialized from year 1000 of the pre-industrial control run. It is important to note that the freshwater flux correction does not depend on the state of the model. Further, the freshwater flux-corrected integration remains fully interactive as the control run, while the mean state is much improved. Our approach introduces some inconsistency, as the freshwater flux correction was estimated using present-day CO_2 -concentration but added to an integration employing pre-industrial CO_2 -concentration. However, pre-industrial SSSs are not available. We assume that the inconsistency in the experimental setup with regard to the CO_2 -concentration does not impact the major results of this study. This is supported by computing the differences in annual-mean SSS between the pre-industrial and a present-day control run, and these differences are much smaller than the SSS biases (not shown).

The area-averaged freshwater flux correction applied to the model amounts to 0.15 Sv, which (in our sign

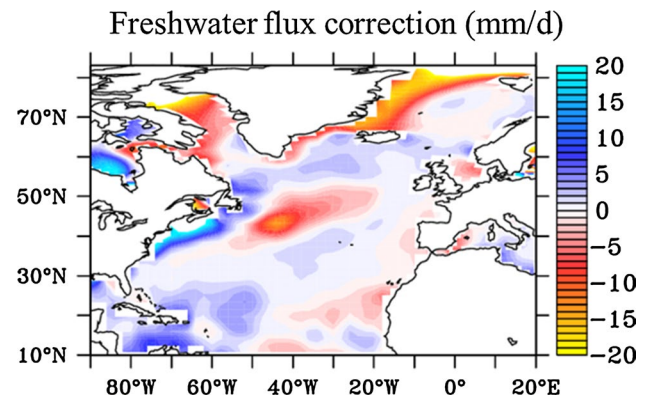
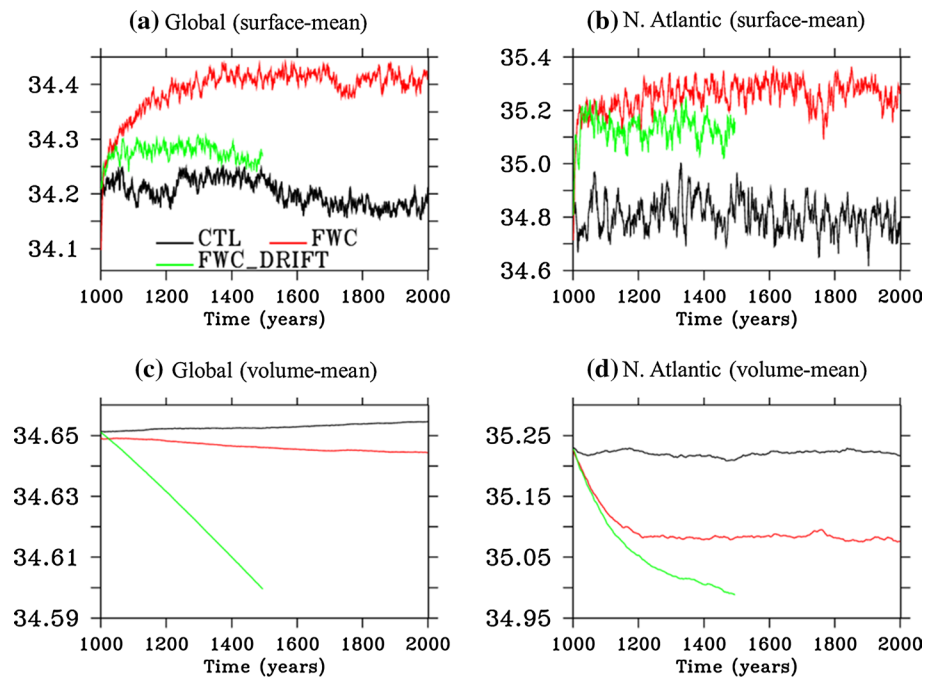


Fig. 1 Annual-mean freshwater flux correction (mm/d) diagnosed from the last 50 years of the 100-yr long run in which the KCM's sea surface salinity (SSS) was restored to Levitus climatology. The area-averaged flux correction amounts to about 0.15 Sv, which means that the ocean gains freshwater

convention) means that the ocean gains freshwater on average. However, the freshwater flux correction depicts significant regional variation (Fig. 1). There is a large freshwater input into the Caribbean, a dipolar structure in the mid-latitudes with a freshwater gain off the east coast of the US and freshwater loss further to the east, and a freshwater loss in most of the subpolar North Atlantic and the Arctic. As will be discussed below, it is this regional variation in the freshwater flux correction that is important in determining the character of the ocean circulation changes.

Sea surface height (SSH) is adjusted every year to compensate for the net freshwater gain introduced by the freshwater flux correction, so that global volume is conserved. This also removes most of the drift in the volume-mean salinity (Fig. 2, compare the green with the red curves). The freshwater flux-corrected integration is labeled FWC and the control run CTL in the figures. There is some initial drift (Fig. 2). Globally averaged SSS equilibrates after about 150 years (Fig. 2a), while SSSs averaged over the North Atlantic after a few decades (Fig. 2b). Volume-mean salinities, however, exhibit a considerably longer adjustment time (Fig. 2c, d) which is on the order of 200 years in the North Atlantic. Relative to the control run, the globally averaged SSS (Fig. 2a) is increased by about 0.2 psu in the integration employing a freshwater flux correction. In the North Atlantic average, there also is an increase of SSS which amounts to about 0.5 psu (Fig. 2b). Volume-mean salinity, in both the global and North Atlantic average (Fig. 2c, d), is lower relative to the control run, indicating the net effect of the freshwater flux correction, which constitutes a freshening of the ocean. After applying the SSH adjustment, global volume-mean salinity exhibits only a small trend of 0.005 psu/1000 years, whereas the drift in North Atlantic volume-mean salinity is negligible. The last 700 years from the

Fig. 2 Temporal evolution of surface-mean and volume-mean salinity (psu). The *left panels (a, c)* depict the time series for the global ocean, the *right panels (b, d)* for the North Atlantic. The control run with the KCM is shown in *black*. The freshwater flux-corrected integration is shown in *red*, and the freshwater flux-corrected integration without the application of the SSH adjustment is shown in *green*



freshwater flux-corrected and SSH-adjusted integration and from the control are used in the analyses shown below (red and black curves in Fig. 2, respectively).

Where possible, observations are used for model comparison. The SSS and SST climatology as well as the mixed layer depth climatology have been taken from NODC (Levitus) World Ocean Atlas 1994 (<http://www.esrl.noaa.gov/psd/data/gridded/data.nodc.woa94.html>). In order to investigate SST variability data from HadISST has been used (Rayner et al. 2003, <http://www.metoffice.gov.uk/hadobs/hadisst/data/download.html>). The long-term mean SSH field has been obtained from AVISO (https://icdc.zmaw.de/ssh_aviso.html). The sea ice concentration climatology has been averaged over the period of 1979–2014 and is from NSIDC (Tonboe et al. 2011, <http://nsidc.org/data/nsidc-0508.html>).

Unless stated otherwise, we use annual-mean data in the subsequent analyses. Statistical significance of correlations is assessed by a *t* test, where the number of degrees of freedom has been estimated from the autocorrelation functions of the corresponding time series. Empirical Orthogonal Function (EOF) analyses have been performed on selected linearly detrended quantities.

3 Results

3.1 Mean state

We first compare the long-term mean SSSs (Fig. 3a, b) and SSTs (Fig. 4a, b) simulated in the two integrations as well as the corresponding biases relative to Levitus

climatology (Figs. 3c, 4c). In contrast to the control run (Fig. 3d) and as expected, the SSS biases in the freshwater flux-corrected integration are relatively small in the North Atlantic (Fig. 3e). Relative to the control run, there is an overall increase in SSS in the Arctic, in the subpolar and mid-latitude North Atlantic (Fig. 3f). A decrease in salinity is observed in the subtropical gyre region. Outside the North Atlantic, there is hardly any change in SSS. We note that the changes in North Atlantic SSS are not necessarily the result of the local freshwater flux correction (Fig. 1). For example, the freshwater flux correction over the Labrador Sea, though small, would support lower SSS in that region, but a strong increase in SSS is simulated relative to the control run (Fig. 3f). This indicates a strong feedback of changes in ocean circulation and/or air–sea interactions, where the latter would result from changes in SST and sea ice. The impact of the freshwater flux correction is not restricted to the surface. A large reduction of salinity biases can be noticed down to 1000 m along 37°W (Fig. S1).

Further, marked changes in North Atlantic SST result when applying a freshwater flux correction (Fig. 4). In particular, the cold SST bias observed in the control run (Fig. 4d) is markedly reduced (Fig. 4e), with an average temperature increase of about 1.5 °C in the region 50°W–10°W and 40°N–60°N and peak warming of up to 5 °C in a zonal band slightly north of 40°N (Fig. 4f). We note the similarity to the pattern shown in Scaife et al. (2011) who employed higher horizontal model resolution to reduce the SST bias. The warming coincides with higher SSS (Fig. 3f), suggesting a northward extension of the subtropical gyre and a more northern position of the North

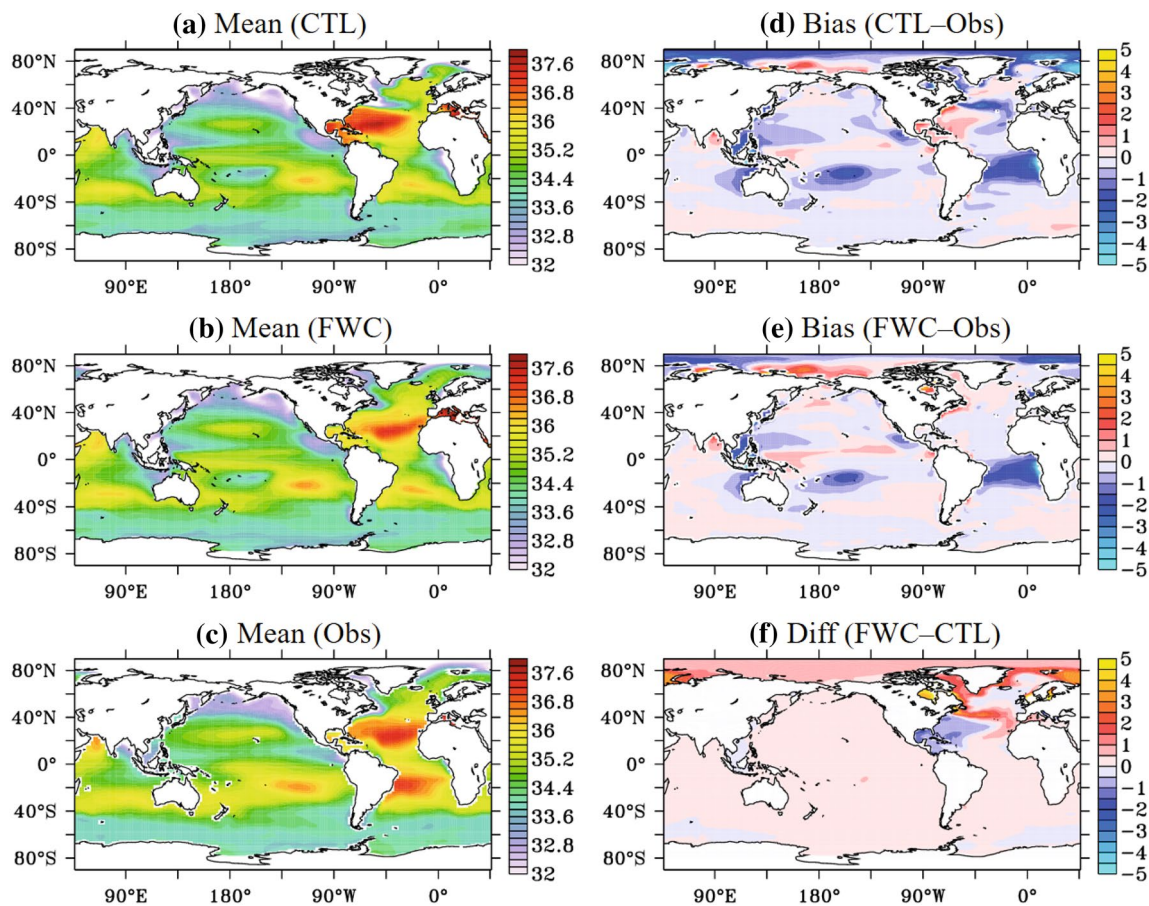


Fig. 3 Long-term annual-mean SSS (psu) in **a** the control run, **b** the freshwater flux-corrected integration, and **c** from Levitus climatology. SSS biases (psu) are depicted in **d** for the control run, **e** the fresh-

water flux-corrected integration, and **f** depicts the difference in SSS between the two integrations

Atlantic Current. The higher North Atlantic SSTs warm the SAT over large regions of the Northern Hemisphere (not shown). Such an impact is known from the positive phase of the AMV (Knight et al. 2005). Outside the North Atlantic, the SST changes are relatively small. There is overall cooling of the Southern Hemisphere, which together with the North Atlantic warming contributes to an interhemispheric dipole pointing to a stronger AMOC, as suggested by Latif et al. (2006) and by a number of climate models (e.g., Drijfhout 2015). The largest surface cooling is found in the Southern Ocean. Finally, subsurface temperature biases are generally reduced when applying a freshwater flux correction (Fig. S2). The cold temperature bias in the mid-latitudes, for instance, is reduced down to about 500 m.

The AMOC strengthens relative to the control run (Fig. 5a) when applying a freshwater flux correction over the North Atlantic (Fig. 5b), as suggested by the aforementioned SST changes. We define an AMOC index as the maximum of the Atlantic meridional overturning streamfunction. This index is enhanced by about 3 Sv in the

freshwater flux-corrected integration relative to that in the control run (see also Fig. 10). The strongest changes are seen in the region 50°N–60°N with values of several Sv at a depth of about 1500 m (Fig. 5c). Moreover, the vertical extent of the North Atlantic Deep Water (NADW) cell becomes larger. Both the stronger AMOC and its larger vertical extent are more realistic in comparison to ocean re-analyses and inverse calculations. The outflow of the NADW at 30°S is only slightly stronger in the freshwater flux-corrected integration, by approximately 1 Sv. Consistent with the stronger AMOC, the northward heat transport is enhanced in the latitude range 30°S–40°N, with largest increases on the order of about 0.1 PW in the subtropical South and North Atlantic (Fig. 6a). Poleward from about 45°N, the northward heat transport in FWC is reduced relative to that in CTL and thus cannot explain the surface warming there. The warmer North Atlantic SSTs in FWC are the result of better representing the North Atlantic Current, and sea ice in the Labrador Sea and Irminger Sea (see below). The reduction in the cold North Atlantic SST bias results in enhanced oceanic heat loss to the atmosphere in

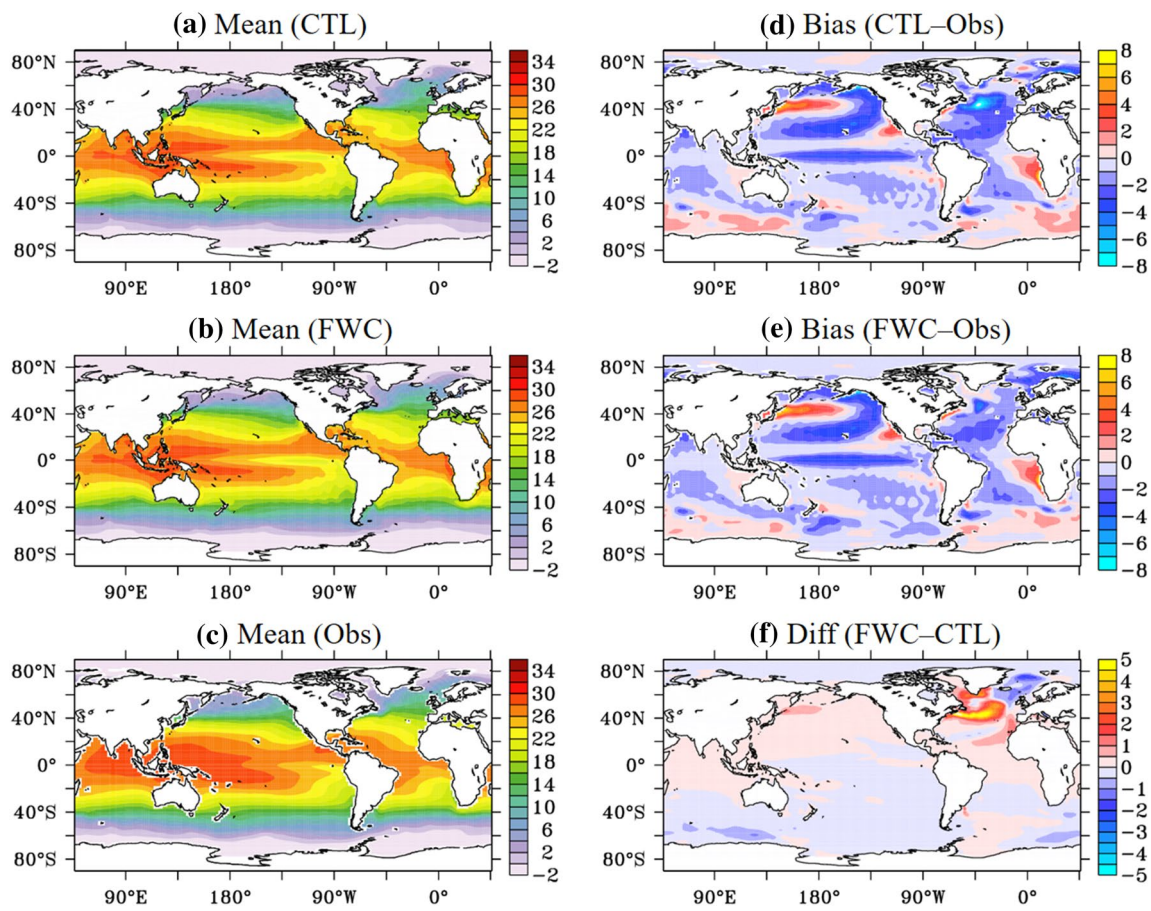


Fig. 4 Long-term annual-mean SST ($^{\circ}\text{C}$) in **a** the control run, **b** the freshwater flux-corrected integration, and **c** from Levitus climatology. SST biases ($^{\circ}\text{C}$) are depicted in **d** for the control run, **e** the fresh-

water flux-corrected integration, and **f** depicts the difference in SST between the two integrations

FWC (Fig. 6b). The stronger AMOC (Fig. 5c) is an interesting result, given that the flux correction provides a net freshwater input to the North Atlantic. If homogeneously distributed that gain would tend to slow the AMOC. Thus, it is the spatial pattern of the freshwater flux correction that matters to AMOC strength.

We use mixed layer depth (MLD) to identify the deep convection sites. The MLDs in the model and the observed MLDs from Levitus' climatology were calculated using a density-based criterion based on 0.01 and 0.125 kg/m^3 , respectively. We repeated the model-MLD calculation using 0.125 kg/m^3 , but the major conclusions are unchanged. The location of the deep convection sites, as expressed by the late winter-mean (JFM) MLD (Fig. 7), is more realistically simulated in the integration employing a freshwater flux correction. In particular, the deep convection site located south of Greenland in the control run (Fig. 7a) is shifted to the west into the Labrador Sea (Fig. 7b, d), which is more in line with Levitus climatology (Fig. 7c). One likely reason for this westward shift is the considerably larger SSSs in the Labrador Sea, with

increases up to 2 psu. We do not discuss here the magnitude of the simulated mixed layer depths which are much larger than those from Levitus climatology, because observational estimates are subject to large uncertainties (see e.g., de Boyer Montégut et al. 2004). This certainly does not exclude the possibility that the model-mixed layer depths are too large.

The simulated time-mean sea surface heights (SSHs, Fig. 8) are compared with those from AVISO averaged over the period 1993–2012. In the control run (Fig. 8a), the SSH pattern exhibits large biases in comparison to that from AVISO (Fig. 8c). A marked improvement is seen in the freshwater flux-corrected integration (Fig. 8b) in which a stronger and more northward reaching subtropical gyre is simulated (Fig. 8d). Further, the circulation is less zonal in the mid-latitudes. The subpolar gyre is less extensive and the SSHs are less deep when applying a freshwater flux correction.

There is a strong decrease up to about 40 % in the sea ice concentration of the Labrador Sea when applying a freshwater flux correction to the model (Fig. 9). The occurrence

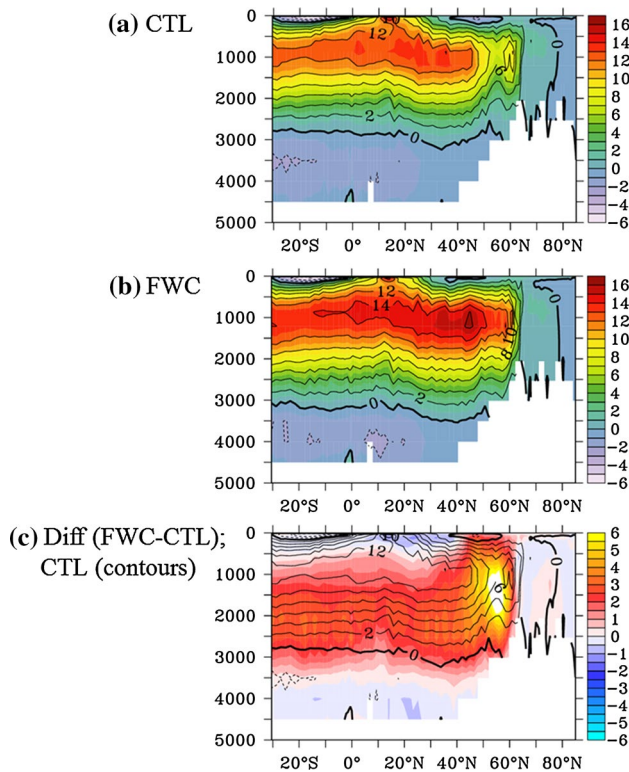
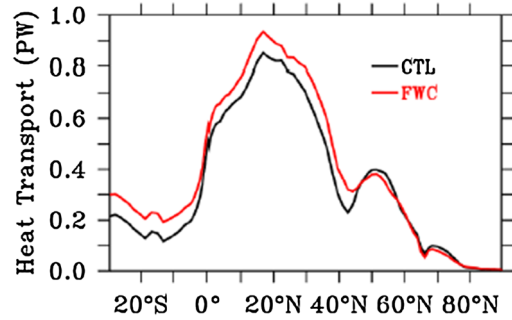


Fig. 5 Long-term annual-mean Atlantic meridional overturning streamfunction (Sv) in **a** the control run (CTL), **b** the freshwater flux-corrected integration (FWC), and **c** the difference between the two (color shading), with contours depicting the meridional overturning streamfunction of CTL

of deep convection in the Labrador Sea (Fig. 7) in that integration is likely due to both reduced sea ice and higher SSSs (Fig. 3), but these two factors are not independent of each other. In the Barents Sea region, the sea ice simulation in the freshwater flux-corrected integration is degraded and the positive sea ice concentration bias enhanced relative to the control run. Thus, the overall representation of Arctic sea ice remains an issue in the KCM. Statistically significant changes in sea level pressure (SLP) relative to the control run are seen globally when applying a freshwater flux correction (Fig. S3f). Over the North Atlantic, the largest change is the reduction of the positive SLP bias in the mid-latitudes (Fig. S3f). This is the region of the largest SST increase (Fig. 4f). The changes in the low-level atmospheric circulation over the North Atlantic are generally statistically significant and represent an improved simulation relative to the control run, and they are consistent with those described by Keeley et al. (2012) and Scaife et al. (2011). Changes in the mean atmospheric circulation will not be discussed any further.

In summary, the freshwater flux correction applied to the KCM over the North Atlantic considerably enhances the simulation of the mean basin-scale circulation of the North

(a) Atlantic Meridional Heat Transport



(b) Atlantic Zonally Integrated Qnet

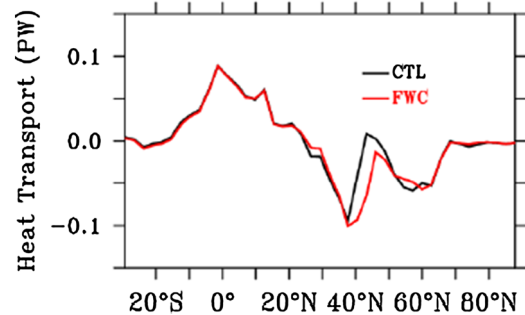


Fig. 6 a The zonally integrated northward heat transport (PW) in the Atlantic in the control run (black) and the freshwater flux-corrected integration (red) and **b** the zonally integrated net surface heat flux in the Atlantic (PW)

Atlantic Ocean and the representation of North Atlantic SSTs, which is a major result of this study. Significant differences between the simulations with and without applying a freshwater flux correction over the North Atlantic are not restricted to the surface and also seen at subsurface levels in the upper kilometer of the North Atlantic, suggesting realistic simulation of North Atlantic SSS is a key to improve climate model simulations of North Atlantic sector mean climate.

3.2 Decadal to multidecadal variability

How are the improvements in the long-term mean ocean circulation of the North Atlantic and in the long-term mean surface climate in the North Atlantic sector reflected in the decadal to multidecadal variability simulated by the model? This is the topic of the remaining part of the results section.

3.2.1 AMOC variability and impact on SAT

An AMOC index is defined as the maximum of the overturning streamfunction at 30°N (Fig. 10). In comparison to the control run (black curve), the AMOC in the freshwater flux-corrected integration is not only stronger (Fig. 5) but

Fig. 7 Long-term late winter-mean (JFM) mixed layer depth (m) in **a** the control run, **b** the freshwater flux-corrected integration, **c** from Levitus climatology, and **d** the difference between the two integrations

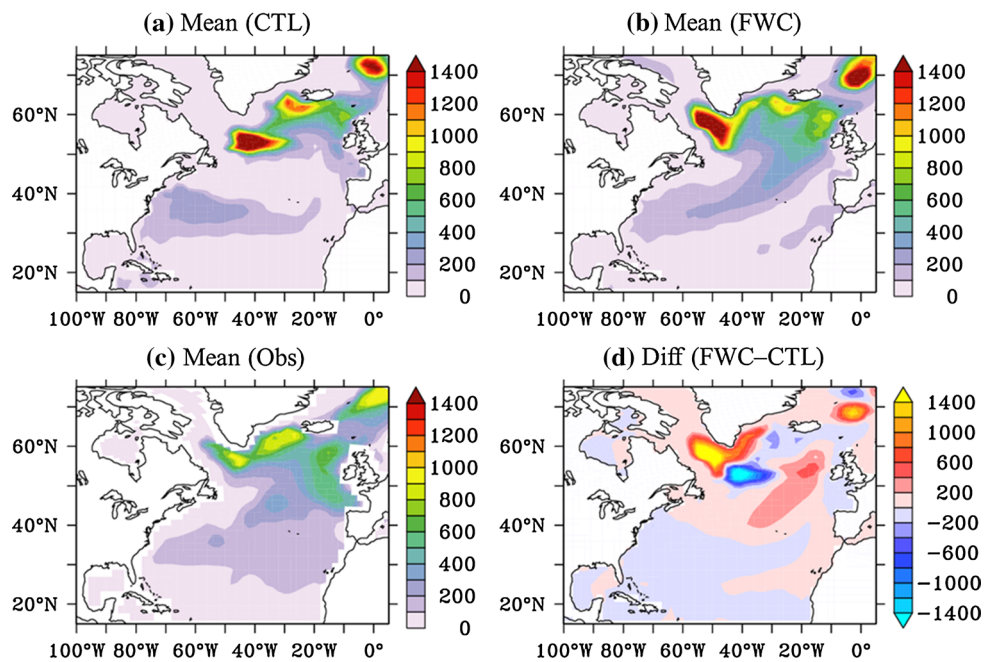
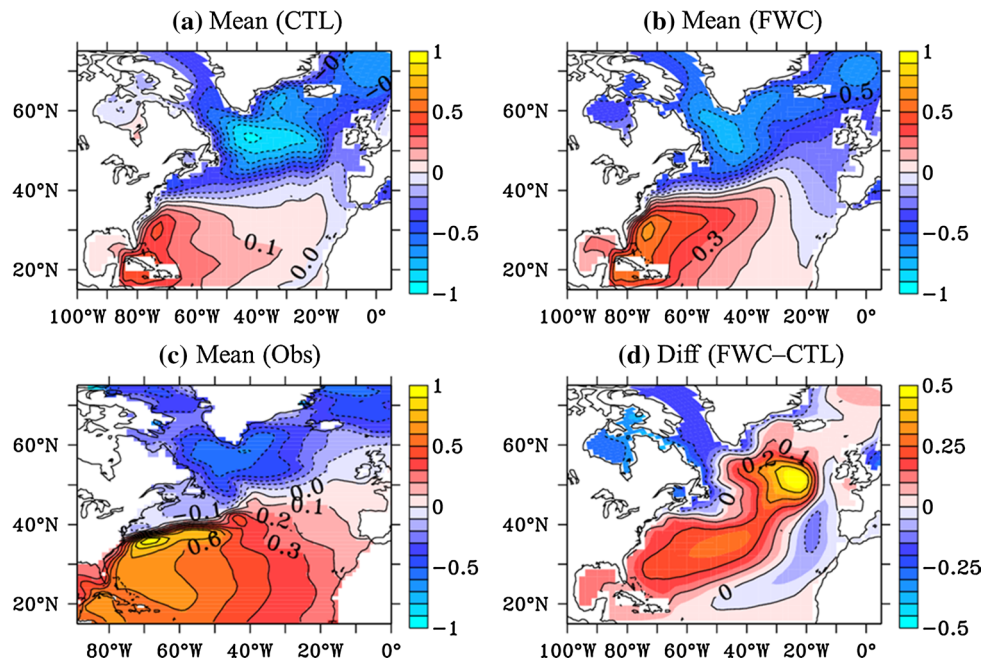


Fig. 8 Long-term annual-mean sea surface height (SSH, m) relative to the global spatial average in **a** the control run, **b** the freshwater flux-corrected integration, **c** from AVISO, and **d** the difference between the two integrations



also exhibits larger decadal to multidecadal variability (red curve). Further, the AMOC index from the freshwater flux-corrected integration appears to be more realistic in comparison to the limited RAPID data (blue curve). We note the large and abrupt transition around model year 1770 (see also Fig. 12b) that is unlike anything seen in the control run but has some similarity to the recently observed drop in AMOC strength (Fig. 10). Using the AMOC index, we explore the relationship of the AMOC to the variability in other quantities. First, the link of the AMOC to Northern

Hemisphere SAT anomalies is investigated by linear regression (Fig. 11). In the freshwater flux-corrected integration, an anomalously strong AMOC is associated with surface warming over most of the Northern Hemisphere (Fig. 11b), which is not the case in the control run which depicts a patchier SAT anomaly pattern (Fig. 11a). Over the North Atlantic, highly significant regressions with explained variances (green contours) up to 30 % are observed in the freshwater flux-corrected integration. Explained variances in the control run are much weaker and amount to less

Fig. 9 Long-term winter-mean (DJFM) sea ice concentration (%) in **a** the control run, **b** the freshwater flux-corrected integration, and **c** from satellite observations. The sea ice concentration biases (%) are depicted in **d** for the control run, **e** the freshwater flux-corrected integration, and **f** depicts the difference between the two integrations. The observations were re-gridded onto the model grid in **d**, **e** to aid comparison

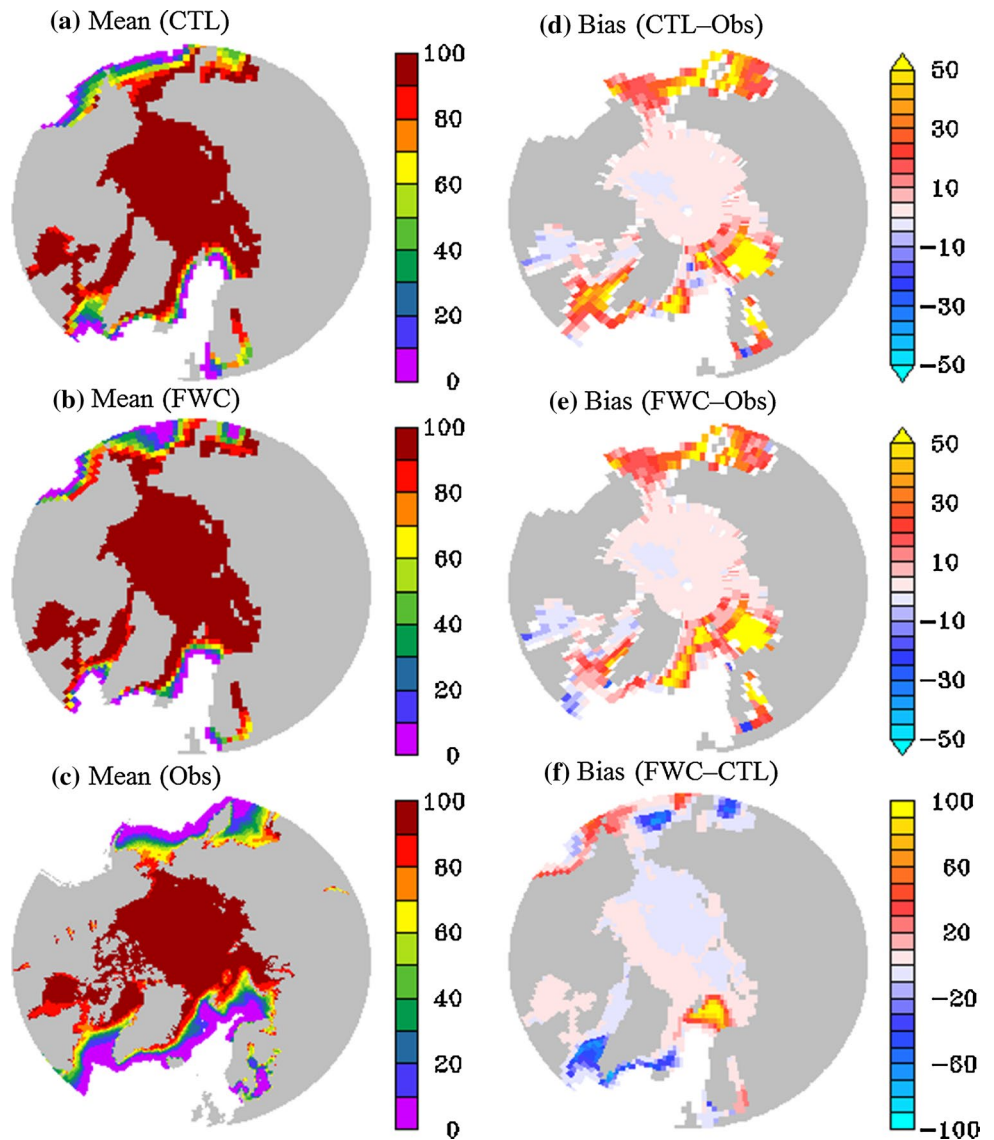
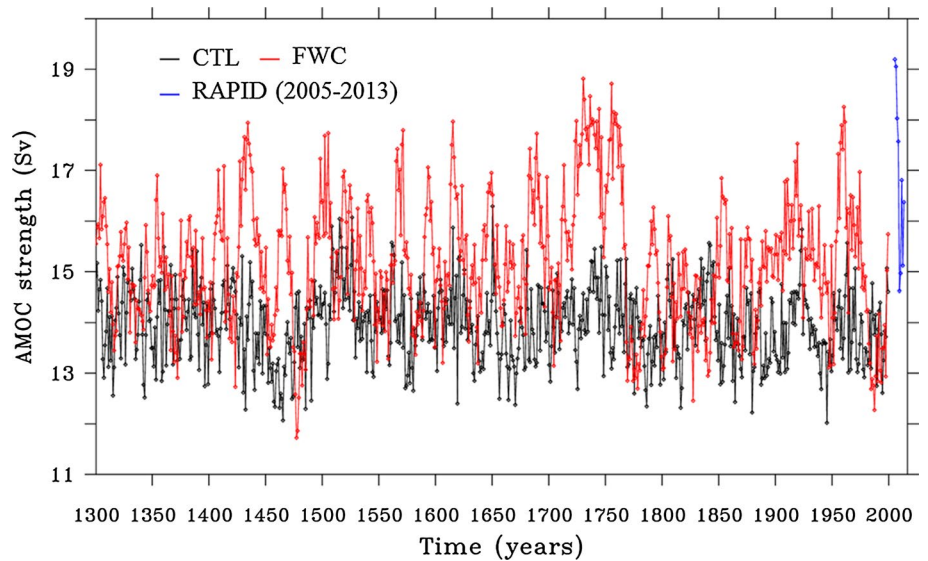


Fig. 10 Time series of the AMOC index (Sv). The *black* curve depicts the AMOC index from the control run, the *red* curve from the integration employing a freshwater flux correction in the North Atlantic. The *blue* curve on the very right side is the AMOC time series at 26.5°N from the RAPID array



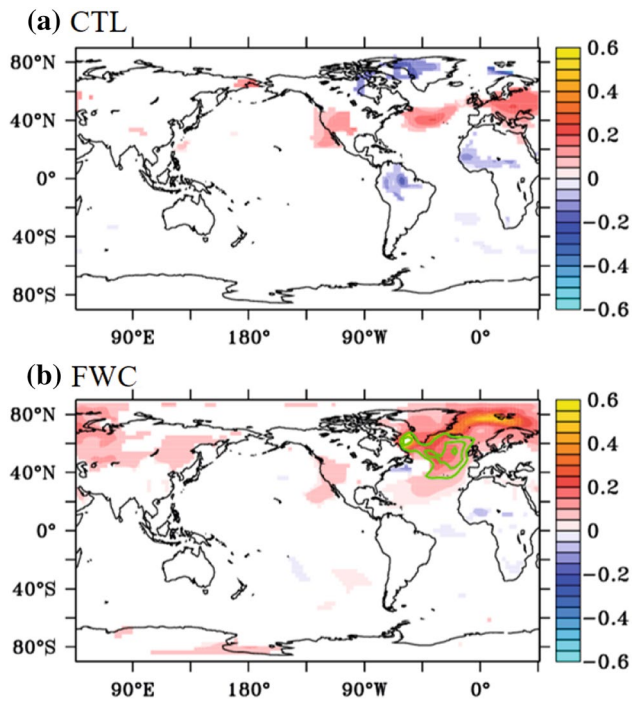


Fig. 11 Local regression coefficients ($^{\circ}\text{C}/\text{Sv}$) of 2 m-temperature anomalies on the AMOC index in **a** the control run and **b** the freshwater flux-corrected integration. Only statistically significant regressions on the 95 %-level are shown. The *green contours* depict explained variance (contour interval is 0.1). Annual-mean data have been used in the calculations

than 10 %. Further, there are hardly any statistically significant SAT anomalies over Eurasia linked to the AMOC in the control run. The hemispheric-scale character of the

Northern Hemisphere SAT pattern simulated in the freshwater flux-corrected integration is consistent with observations (Knight et al. 2005).

3.2.2 AMV

We computed the leading EOFs of North Atlantic SSTs from observations and the two model simulations (Fig. 12). The leading EOF of North Atlantic SST variability well represents the AMV in all three datasets. The variance accounted for by the leading SST-EOF amounts to 27 % when employing a freshwater flux correction over the North Atlantic, as opposed to 18 % in the control run. This is lower in comparison to the variance explained by the leading SST-EOF calculated from observations amounting to almost 35 %. We note that the latter value may be subject to large uncertainty given the short instrumental record. Further, the AMV variance in the observations might have been increased by changes in external forcings, making strict comparison with our simulations, which only contain internal variability, less appropriate.

All three EOF patterns (upper panels in Fig. 12) depict a significant monopolar component, and the corresponding Principal Components (PCs, lower panels) exhibit strong decadal to multidecadal variability. The latter is considerably stronger in FWC in comparison to CTL. In the control run (Fig. 12a), the strongest SST anomalies are simulated in the mid-latitudes. In the freshwater flux-corrected integration (Fig. 12b), the AMV, as expressed by the leading EOF, is more realistically simulated than that in the control run. Consistent with observations (Fig. 12c), the strongest

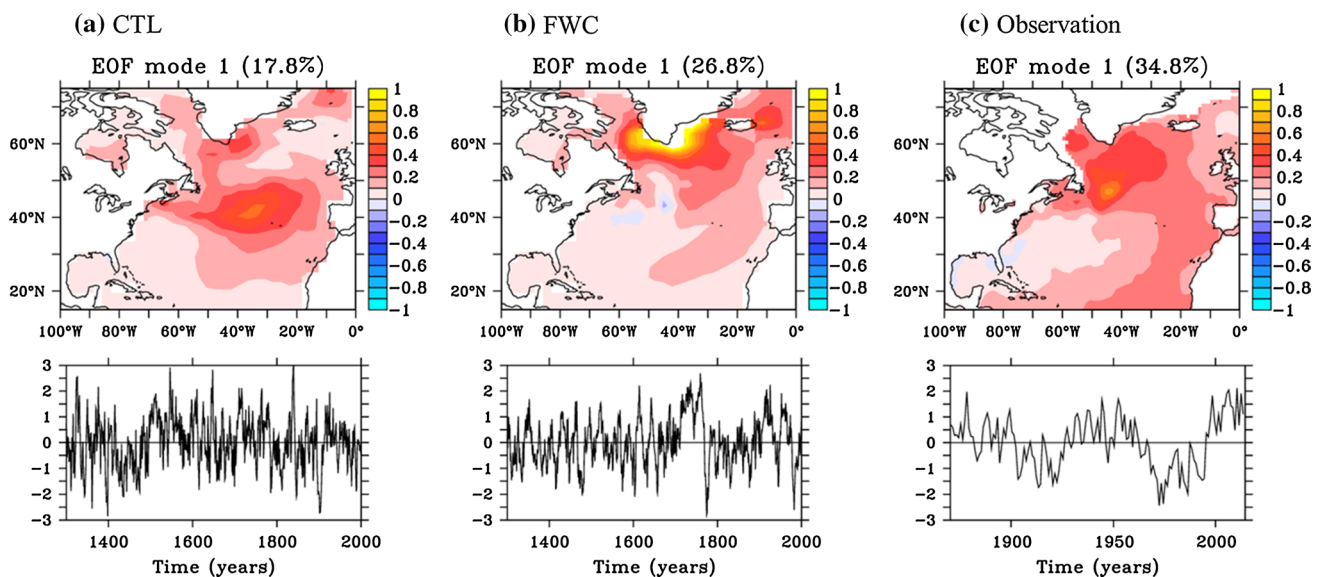


Fig. 12 The leading EOF mode ($^{\circ}\text{C}$) of SST and the corresponding PC (normalized) calculated from **a** the control run, **b** the freshwater flux-corrected integration, and **c** observations (please note the different timescale in the PCs). Annual-mean data have been used in the calculations

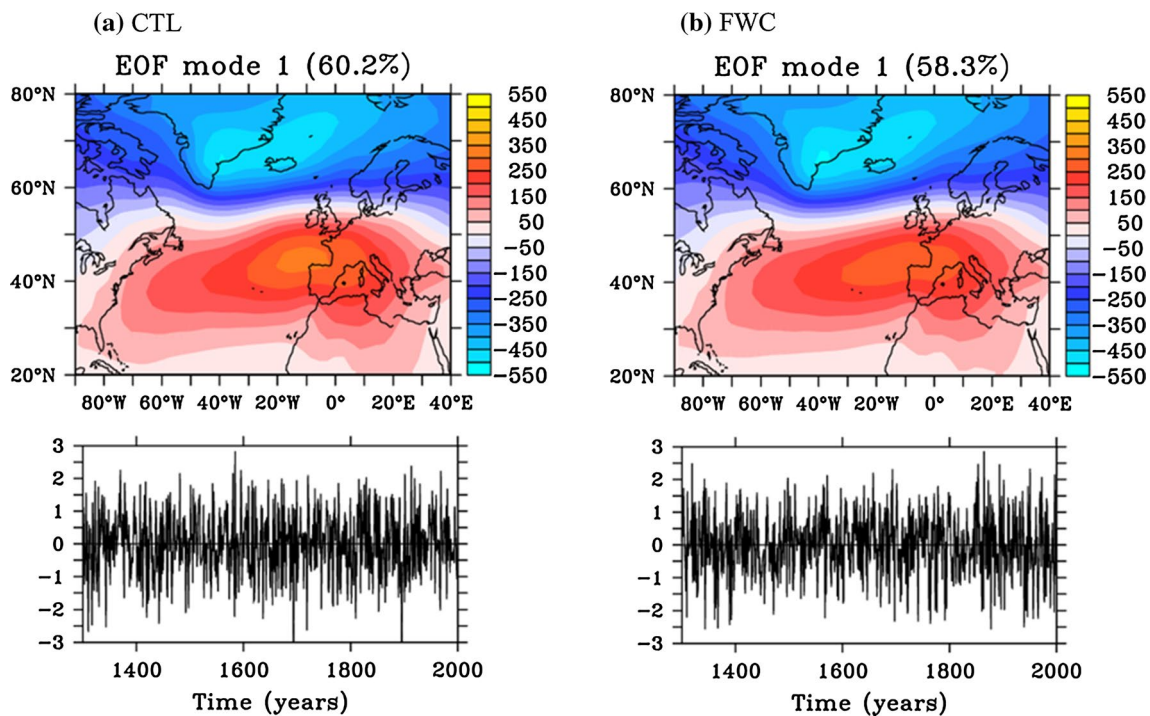


Fig. 13 The leading EOF mode (Pa) and the corresponding PC (normalized) of SLP calculated from **a** the control run and **b** the freshwater flux-corrected integration. Winter (DJFM)-mean data have been used in the calculations

SST anomalies are simulated in the northern North Atlantic, but the SST anomalies south of Greenland are overly large. A minimum is seen in the western part of the subtropical gyre, again consistent with observations.

3.2.3 NAO/AMOC link

In both integrations, the leading EOF mode of sea level pressure (SLP) variability is the North Atlantic Oscillation (NAO, Fig. 13). It does not significantly differ between the two integrations in terms of either spatial pattern or explained variance. However, relative to the SLP-PC1 from CTL, the SLP-PC1 from FWC features consistently more power at decadal timescales, which was derived from computing the corresponding power spectra (Fig. S6a). This suggests an influence of the changed decadal SST variability characteristics in FWC on the low-level atmospheric circulation over the North Atlantic in that integration.

The AMOC relationship to the NAO is stronger in the freshwater flux-corrected integration relative to that in the control run. This can be inferred from the cross-correlation function of the NAO index with the AMOC index (Fig. 14a, b). In comparison to the control run (Fig. 14a) depicting only marginally significant correlations, the cross-correlation function computed from the freshwater flux-corrected integration (Fig. 14b) shows a clear and relatively broad

peak which is highly significant. The time lag of several years seen in both integrations indicates that variability of the NAO leads that of the AMOC. Spectral analyses reveal that the spectrum of the NAO-index (as defined by SLP-PC1 shown in Fig. 13) is almost white in both FWC and CTL, while that of the AMOC is red in the two simulations (Fig. S6). The overall small correlations in Fig. 14a, b is not surprising given the large year-year variability of the NAO.

3.2.4 AMV/AMOC link

The AMV/AMOC relationship, as investigated by correlating SST-PC1 with the AMOC index, is much more robust in the freshwater flux-corrected integration in comparison to that in the control run (Fig. 14c, d): the maximum correlation in the former amounts to about 0.6 as opposed to about 0.3 in the latter. We verified this result by using another SST index defined as the annual-mean SST anomalies averaged over the region 40°N–60°N and 50°W–10°W. This region has been suggested as the region of strongest AMOC influence on SST (Latif et al. 2004). Largest cross-correlations between the area-averaged North Atlantic SST anomalies and the AMOC index amount to about 0.7 and 0.3 in the freshwater flux-corrected integration and in the control run, respectively (not shown).

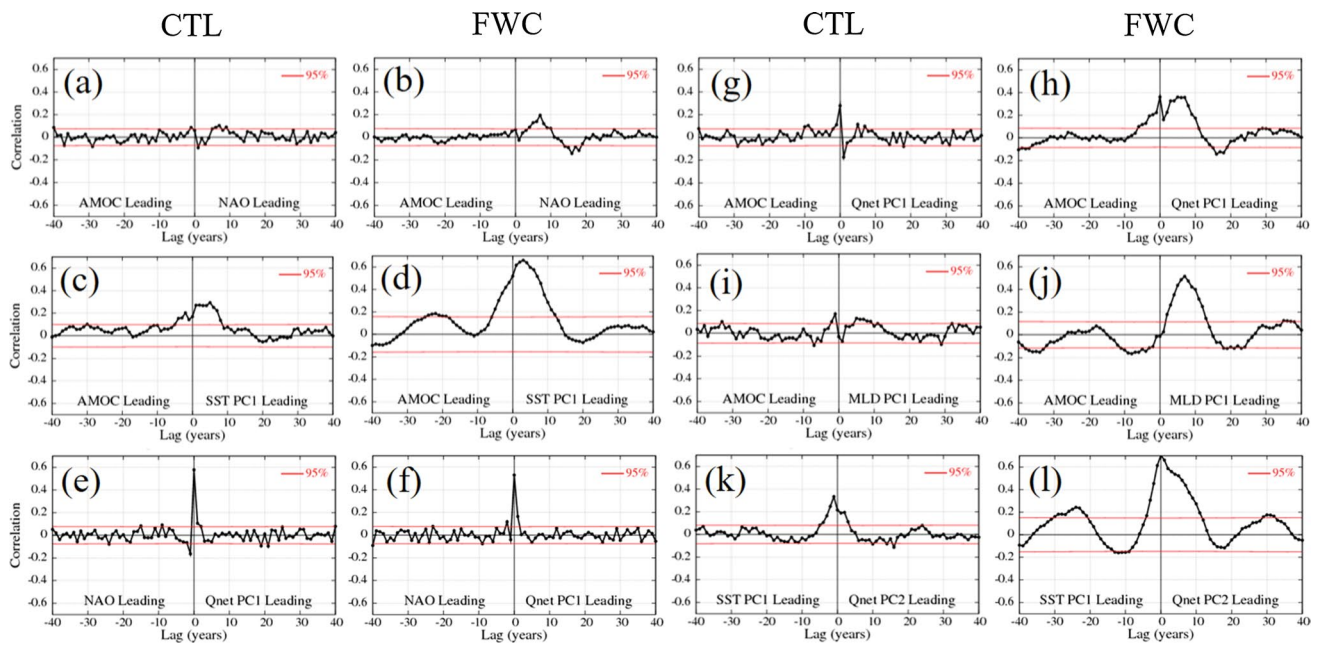


Fig. 14 Cross-correlations as a function of the time lag (yr) of **a, b** the NAO index with AMOC index, **c, d** the AMOC index with SST-PC1, **e, f** the NAO index with heat flux-PC1, **g, h** the AMOC index with heat flux-PC1, **i, j** the AMOC index with MLD-PC1, and **k, l** SST-PC1 with heat flux-PC2. *Panels (a, c, e, g, i, k)* depict the

cross-correlations for the control run, and *panels (b, d, f, h, j, l)* the cross-correlations for the freshwater flux-corrected integration. The *red lines* depict the 95 %-confidence limits. The different number of degrees of freedom explains the different confidence limits

The maximum correlation is found when SST-PC1 leads the AMOC index by a few years (Fig. 14c, d). The pattern of SST-EOF1 is not orthogonal to the tripolar SST anomaly pattern prevailing at interannual timescales, which confuses cause and effect. The NAO, through changes in surface heat flux, drives both the tripolar SST anomaly pattern and the AMOC, and the AMOC (with a time delay) feeds back on the SST. The time lag between the North Atlantic SST and the AMOC index almost vanishes when using the area-averaged North Atlantic SST anomaly index (not shown). In order to further investigate the AMOC influence on the SST, we repeated the cross-correlation analysis with band-pass filtered data retaining variability with periods between 30 and 60 years (Fig. S4). While in the control run, the SST index still leads the AMOC index by about 5 years (Fig. S4a), the AMOC index leads the SST index in the freshwater flux-corrected integration by a couple of years (Fig. S4b). This result has been also obtained from applying cross-wavelet analysis (not shown). Finally, an oscillatory behavior with a multidecadal period can be inferred from the cross-correlation functions between SST-PC1 and the AMOC index (Fig. 14c, d). In the control run, however, correlations are relatively low at all lags rendering the cross-correlation function relatively flat, whereas in the freshwater flux-corrected integration, the magnitude of the correlations is rather high and the periodicity obvious.

3.2.5 Heat flux forcing of the AMOC

The NAO mostly impacts the AMOC through its impact on the surface heat fluxes. We performed an EOF analysis on the net surface heat fluxes (Fig. 15) to further investigate this relationship. In both integrations, the PC of the leading heat flux EOF mode, heat flux-PC1, is well correlated with the NAO index at zero lag (Fig. 14e, f); and the correlations quickly drop off with time lag. The EOF patterns are rather similar (Fig. 15a, b). However, there is one major difference between them: the heat flux anomalies over the Labrador Sea linked to heat flux-EOF1 are considerably larger in the freshwater flux-corrected integration compared to those in the control run.

The fluxes associated with heat flux-EOF1 have the potential to stochastically force decadal and longer time-scale variability of the AMOC through their influence on deep convection (see e.g., Latif 2013 for a review), as the heat flux variability primarily occurs over the major deep convection sites (Fig. 7). We correlated heat-flux PC1 with the AMOC index (Fig. 14g, h). There is a clear connection between the two time series in the freshwater flux-corrected integration, indicating the heat fluxes drive the AMOC with a lead time of several years. This connection, though present, is much weaker in the control run. We speculate that the more robust forcing of the AMOC by the surface heat

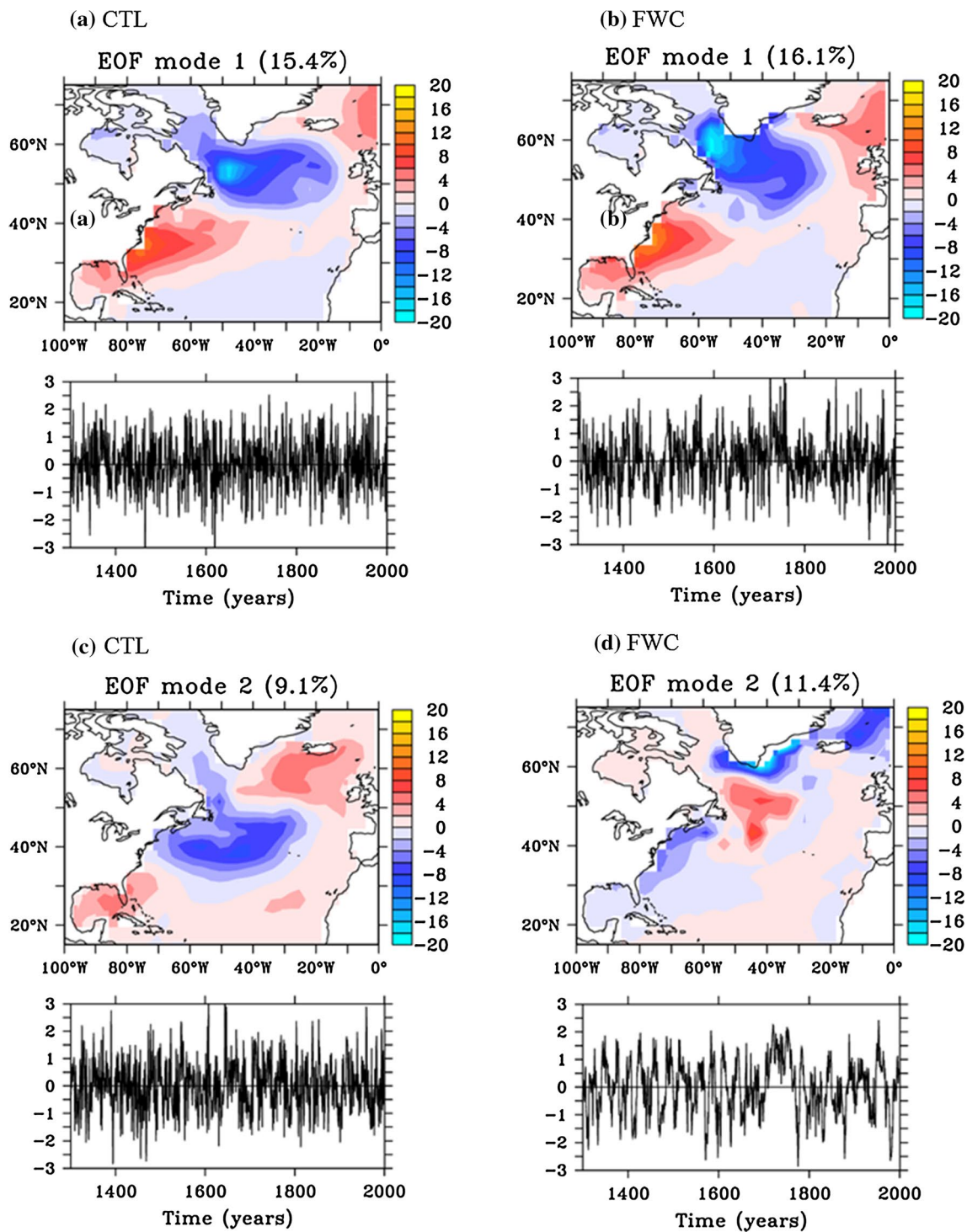


Fig. 15 The two leading EOF modes (Wm^{-2}) and the corresponding PCs (normalized) of the net heat flux in (a, c) the control run and (b, d) the freshwater flux-corrected integration. Annual-mean data have been used in the calculations

fluxes, associated with heat flux-EOF1, in the freshwater flux-corrected integration is a consequence of the strongly reduced sea ice concentration in the Labrador Sea.

We next performed an EOF analysis on the late winter (JFM) mixed layer depths. The variability associated

with MLD-EOF1 is large in those regions (Fig. 16a, b) where the heat flux variability linked to heat flux-EOF1 is large too (Fig. 15a, b). In the control run, the mixed layer depth variability linked to MLD-EOF1 is centered south of Greenland in the open ocean near 55°N and 40°W. In

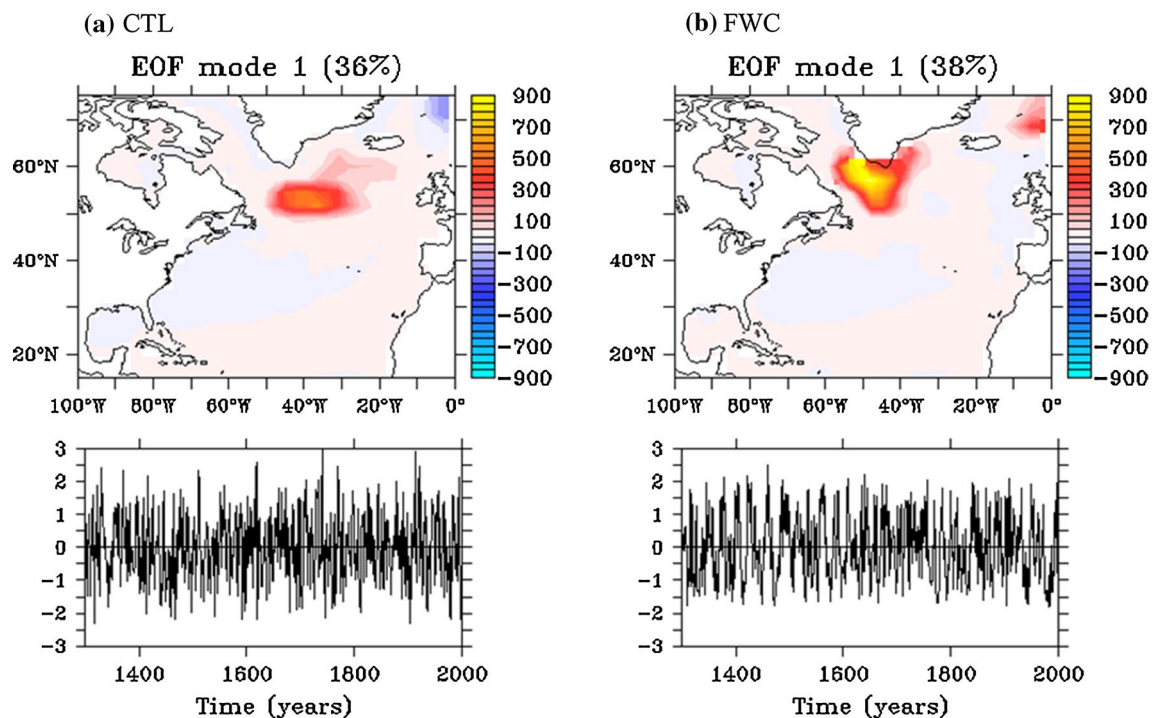


Fig. 16 The leading EOF mode (m) and the corresponding PC (normalized) of mixed layer depth (MLD) in **a** the control run and **b** the freshwater flux-corrected integration. Late winter-mean (JFM) data have been used in the calculations

contrast, the strongest MLD signal associated with MLD-EOF1 in the freshwater flux-corrected integration is shifted to the northwest and located in the Labrador Sea, consistent with observations (e.g., Carton et al. 2008). We computed the cross-correlations of MLD-PC1 with the AMOC index. In both integrations, highest correlations are found when variability associated with MLD-EOF1 leads the AMOC index by about 5 years (Fig. 14i, j). Again and consistent with the other cross-correlation analyses presented above, the correlations are much stronger in the freshwater flux-corrected integration than that in the control run.

3.2.6 Negative heat flux feedback

The second EOF, heat flux-EOF2, is discussed next (Fig. 15c, d). In both integrations, loadings are large and negative in those regions where the SST anomalies associated with SST-EOF1 are large and positive, but these regions strongly differ between CTL and FWC (Fig. 12). The principal components, SST-PC1 and heat flux-PC2, are positively correlated (Fig. 14k, l). Thus, SST variability in the regions of strongest SST variability is damped by the heat fluxes and thus controlled by ocean dynamics. In the control run, for example, SST-EOF1 depicts largest loadings in the mid-latitudes (Fig. 12b), and this is the region where the heat flux anomalies associated with heat

flux-EOF2 also depict strong signals (Fig. 15c). In the freshwater flux-corrected integration, the strong subpolar North Atlantic SST anomalies associated with SST-EOF1 (Fig. 12b) coincide with the strong negative anomalies in heat flux-EOF2 (Fig. 15d). The magnitude of the correlations between SST-PC1 and heat flux-PC2 (Fig. 14k, l) in the freshwater flux-corrected integration is considerably larger than that in the control run. Moreover, heat flux-PC2 from the freshwater flux-corrected integration depicts strong decadal to multidecadal variability and relatively little interannual variability, while the interannual variability is much more prominent in heat flux-PC2 from the control run (Fig. 15c, d).

3.2.7 Gyre circulation/AMOC link

We also study the relationship between the gyre circulation and AMOC variability. The leading EOF of the barotropic streamfunction, PSI-EOF1, calculated from the control run (Fig. 17a) and accounting for about 28 % of the variance, is known as the intergyre gyre (Marshall et al. 2001). The intergyre gyre is a gyre anomaly that straddles the climatological-mean confluence of the subtropical and subpolar gyres and is driven by meridional shifts in the wind pattern associated with fluctuations of the NAO. The corresponding principal component, PSI-PC1, is dominated

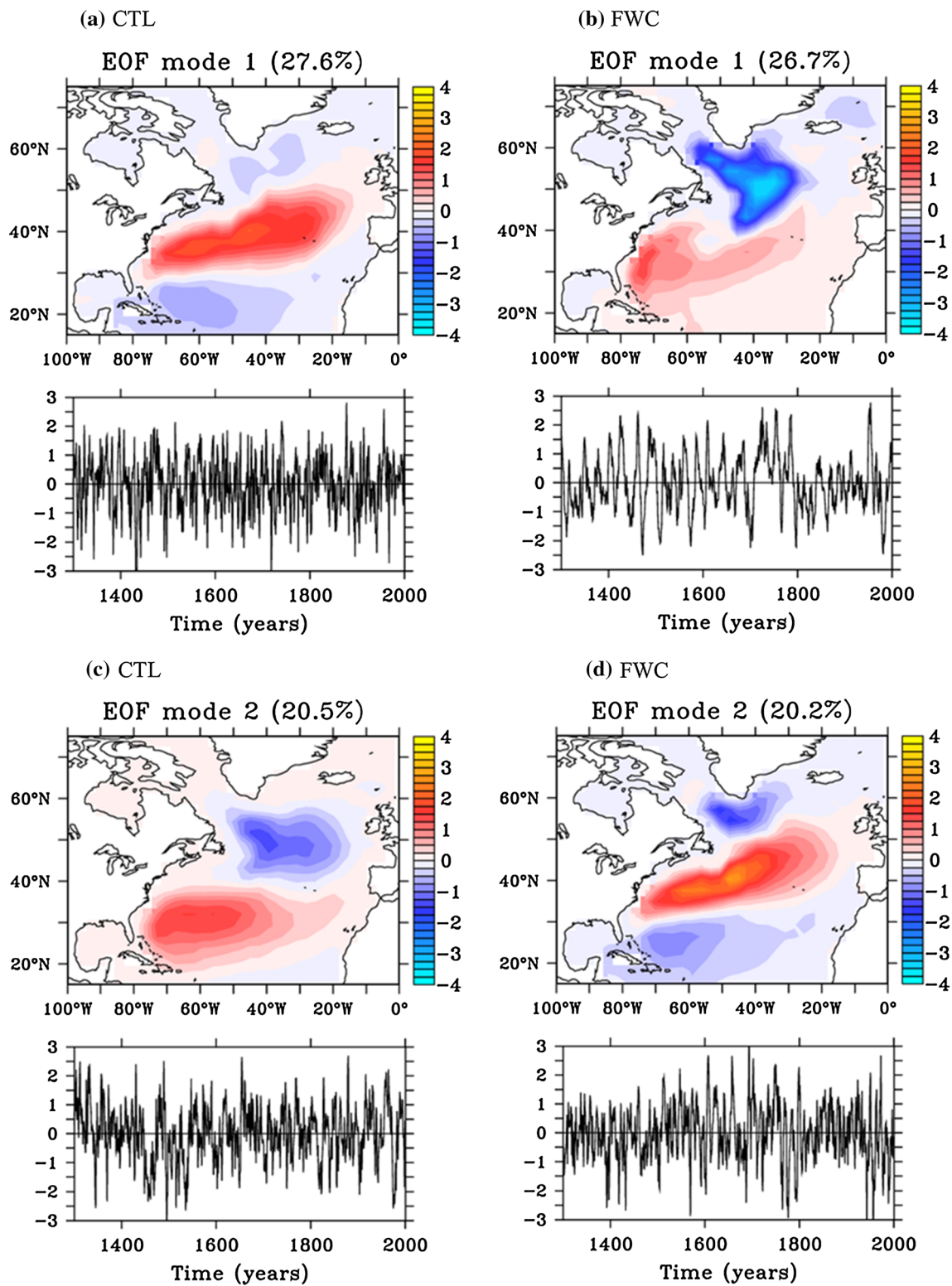
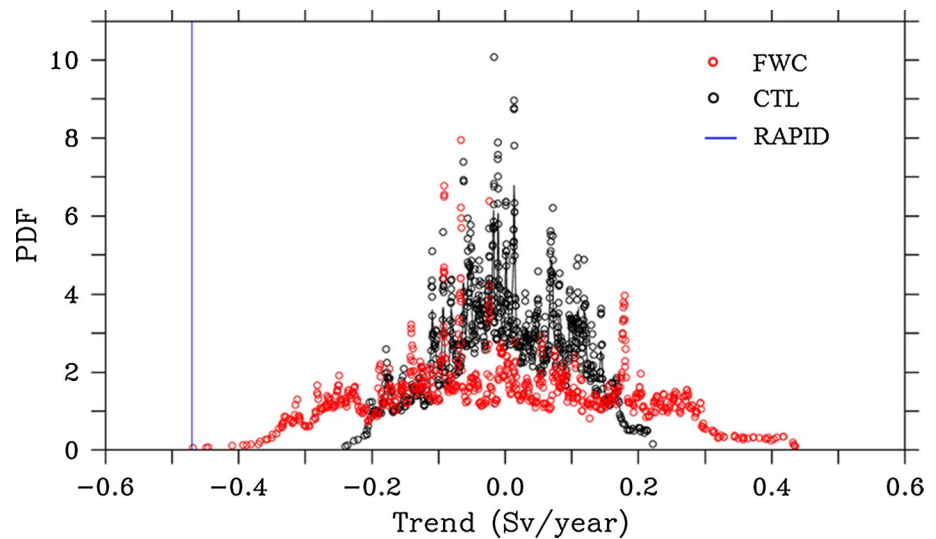


Fig. 17 The two leading EOF modes (Sv) and the corresponding PCs (normalized) of the barotropic streamfunction in **a**, **c** the control run and **b**, **d** in the freshwater flux-corrected integration. Annual-mean data have been used in the calculations

Fig. 18 Distribution of (non-overlapping) 9-yr trends (Sv/year) calculated from the control run (*black symbols*) and the freshwater flux-corrected integration (*red symbols*). The observed 9-yr trend 2005–2013 from RAPID is shown by the *blue line*. Annual-mean data have been used in the calculations



by interannual variability and exhibits a strong correlation (~ 0.6) with the NAO-index at zero lag, with the correlation quickly diminishing with time lag (Fig. S5a). The second EOF of the barotropic streamfunction (Fig. 17c), PSI-EOF2, calculated from the control run and explaining about 21 % of the variance, has large loadings in both the subpolar gyre region and in the subtropical gyre region. The corresponding principal component, PSI-PC2, like PSI-PC1, is rather noisy. Both PSI-PC1 and PSI-PC2 are not well correlated with the AMOC index (Fig. S5c). Thus in the control run, variability of the barotropic streamfunction is hardly linked to the AMOC.

This dramatically changes in the freshwater flux-corrected integration. The first EOF in that integration, PSI-EOF1 (Fig. 17b), accounting for about 27 % of the variance depicts largest loadings in the subpolar gyre region. PSI-PC1 from the freshwater flux-corrected integration is strongly correlated (~ 0.7) with the AMOC index, with PSI-PC1 leading by several years (Fig. S5b). Further, PSI-PC1 exhibits strong decadal variability, in contrast to the PCs of the two leading EOFs from the control run. Thus, in the freshwater flux-corrected integration, there is a clear link of the variability in the subpolar gyre to the AMOC, which is not the case in the control run. The huge difference in the subpolar gyre/AMOC relationship in the two integrations may help to understand the large spread among climate models concerning the link between the two types of circulations.

The second EOF mode obtained from the freshwater flux-corrected integration, PSI-EOF2, explaining about 20 % of the variance is the intergyre gyre. Its PC, PSI-PC2, is strongly correlated with the NAO index at zero-lag (Fig. S5d). Overall, the cross-correlation function is similar to that of PSI-PC1 with the NAO index in the control run (Fig. S5a).

4 Summary and discussion

We have investigated the impacts of correcting North Atlantic sea surface salinity (SSS) biases on the ocean circulation of the North Atlantic and on North Atlantic sector mean climate and climate variability in the Kiel Climate Model (KCM). Bias reduction was achieved by applying a freshwater flux correction over the North Atlantic to the model. Impacts of the freshwater flux correction are strong and not only restricted to the sea surface, with significant changes in the subsurface ocean down to about 1000 m. The changes generally constitute an improvement in comparison with a control run without employing the correction. Examples of improvements are the Atlantic Meridional Overturning Circulation (AMOC), the gyre circulation, and North Atlantic SST and subsurface temperature. Further, the link between the North Atlantic Oscillation (NAO) and the AMOC is strengthened in the freshwater flux-corrected integration, which is likely due to a better representation of the deep convection site in the Labrador Sea that leads to a larger sensitivity of deep water formation in the subpolar North Atlantic to NAO-related surface heat flux forcing. Moreover, the Atlantic Multidecadal Variability (AMV), the leading mode of decadal North Atlantic SST variability, is more realistically simulated in the model, when flux-correcting North Atlantic SSSs. In particular, the link between the AMOC and the AMV becomes more robust. This is supported by cross-spectral and cross-wavelet analyses performed on the AMOC index and North Atlantic SST index (not shown). For example, on decadal timescales, there is hardly any statistically significant coherence above the 95 %-level in the control run, while in the freshwater flux-corrected integration there is a plateau of statistically significant coherence at periods

between about 30 and 60 years where the AMOC index is leading the SST index.

We conjecture that in climate models with similar SSS biases as those observed in the KCM, the influence of the AMOC on North Atlantic SST and in turn Northern Hemisphere SAT may be significantly underestimated. This could lead to reduced climate variability in the North Atlantic sector and possibly also of climate variability outside the North Atlantic sector (Zhang and Delworth 2006). Thus, the skill of decadal climate prediction may benefit, through a stronger connection between the AMOC and North Atlantic SST, from alleviating North Atlantic SSS biases. It should be noted that the root cause of the North Atlantic SST bias may be of ocean dynamical origin and due to the incorrect path of the North Atlantic Current. Scaife et al. (2011) managed to alleviate this problem in their model by upgrading to a version with improvements that included a much higher ocean resolution. We also correct the path of the North Atlantic Current in the freshwater flux-corrected integration, which in turn considerably improves simulation of North Atlantic SST.

The level of AMOC variability appears to be influenced by the North Atlantic SSS biases. Decadal to multi-decadal AMOC variability considerably intensifies in the KCM when applying a freshwater flux correction over the North Atlantic. Moreover, the impact of AMOC changes on Northern Hemisphere surface climate is also enhanced. This is important in the estimation of the decadal predictability potential in the North Atlantic sector. We additionally show in Fig. 10 the overturning time series from the RAPID array during 2005–2013 (blue curve), providing an observational estimate of the range of AMOC strength at 26.5°N. The recently observed strong downward trend in the AMOC-strength is unusual but not exceptional in comparison to the 9-yr trends simulated in the freshwater flux-corrected integration. In that integration (red time series in Fig. 10), strong and fast AMOC-strength changes of the order of several Sverdrup can happen within a decade (e.g., around model year 1750). Such fast trends in AMOC-strength are not observed in the control run (black time series in Fig. 10). In fact, large differences exist between the 9-yr (non-overlapping) trend distributions of the AMOC indices from the control run and flux-corrected integration (Fig. 18). We find one (downward) 9 yr-trend in the distribution of the flux-corrected integration (red symbols) that depicts the same magnitude as the recent observed trend (blue vertical line) and another two that come close. Such fast 9-yr trends in AMOC-strength are not simulated in the control run (black symbols). This result demonstrates a strong dependence of decadal to multidecadal AMOC variability on North Atlantic SSS biases. High-frequency (interannual) variability, on the other hand, is reduced in the freshwater flux-corrected integration in comparison to

that in the control run, so that the slope of the spectrum of the AMOC index is increased (Fig. S6b). Overall, it seems that AMOC variability and related impacts can be more realistically simulated in climate models when strongly reducing North Atlantic SSS biases either by means of flux correction or by improving the model physics.

Obviously, the large SSS biases in the North Atlantic observed in climate models may have far reaching consequences for the circulation of the North Atlantic. The interpretation of subpolar gyre-strength reconstructions from proxy records as AMOC variability is another example. Whereas the freshwater flux-corrected version of the KCM depicts a robust link between subpolar gyre variability and AMOC variability, the uncorrected model version does not simulate a clear relationship between the two circulation patterns. This is important when investigating paleo-climatic records. Interpretation of subpolar gyre-strength variability reconstructed from proxy data in terms of AMOC variability will critically depend on which model is applied.

Finally, the KCM results suggest that a regional freshwater flux correction may serve as an interim solution to enhance decadal prediction in the North Atlantic sector, as long as SSS biases are overly large in climate models. We conclude this from the fact that the AMV is, in comparison to that in the control run, more realistically simulated in the freshwater flux-corrected version of the KCM, both in terms of its spatial pattern and timescale.

Acknowledgments This work was supported by the Excellence Cluster “Future Ocean” of DFG, BMBF-funded project RACE (No. 03F0651B) and the EU-funded project NACLIM (grant agreement No. 308299). The climate model integrations were performed at the Computing Center of Kiel University and at DKRZ Hamburg.

References

- Ba J et al (2013) A mechanism for Atlantic multidecadal variability in the Kiel Climate Model. *Clim Dyn* 41:2133–2144. doi:[10.1007/s00382-012-1633-4](https://doi.org/10.1007/s00382-012-1633-4)
- Ba J et al (2014) A multi-model comparison for Atlantic multidecadal variability. *Clim Dyn* 43:2333–2348. doi:[10.1007/s00382-014-2056-1](https://doi.org/10.1007/s00382-014-2056-1)
- Carton JA, Grodsky SA, Liu Hailong (2008) Variability of the oceanic mixed layer, 1960–2004. *J Climate* 21:1029–1047. doi:[10.1175/2007JCLI1798.1](https://doi.org/10.1175/2007JCLI1798.1)
- de Boyer Montégut C, Madec G, Fischer AS, Lazar A, Iudicone D (2004) Mixed layer depth over the global ocean: an examination of profile data and a profile-based climatology. *J Geophys Res* 109:C12003. doi:[10.1029/2004JC002378](https://doi.org/10.1029/2004JC002378)
- Delworth TL, Mann ME (2000) Observed and simulated multidecadal variability in the northern hemisphere. *Clim Dyn* 16:661–676
- Delworth TL, Rosati A, Anderson W et al (2012) Simulated climate and climate change in the GFDL CM2. 5 high-resolution coupled climate model. *J Climate* 25:2755–2781. doi:[10.1175/jcli-d-11-00316.1](https://doi.org/10.1175/jcli-d-11-00316.1)
- Drews A, Greatbatch RJ, Ding H et al (2015) The use of a flow field correction technique for alleviating the North Atlantic cold

- bias with application to the Kiel Climate Model. *Ocean Dyn* 65:1079–1093. doi:[10.1007/s10236-015-0853-7](https://doi.org/10.1007/s10236-015-0853-7)
- Drijfhout S (2015) Competition between global warming and an abrupt collapse of the AMOC in Earth's energy imbalance. *Sci Rep* 5:14877. doi:[10.1038/srep14877](https://doi.org/10.1038/srep14877)
- Flato G et al (2013) Evaluation of climate models. In: Stocker TF, Qin D, Plattner G-K, Tignor M, Allen SK, Boschung J, Nauels A, Xia Y, Bex V, Midgley PM (eds) *Climate change 2013: the physical science basis. Contribution of working group I to the fifth assessment report of the intergovernmental panel on climate change*. Cambridge University Press, Cambridge
- Gulev SK, Latif M, Keenlyside NS, Koltermann KP (2013) North Atlantic Ocean control on surface heat flux at multidecadal time-scales. *Nature* 499. doi:[10.1038/nature12268](https://doi.org/10.1038/nature12268)
- Hofmann M, Rahmstorf S (2009) On the stability of the Atlantic meridional overturning circulation. *PNAS* 49. doi:[10.1073/pnas.0909146106](https://doi.org/10.1073/pnas.0909146106)
- Hurrell JW (1995) Decadal trends in the North Atlantic Oscillation regional temperatures and precipitation. *Science* 269:676–679
- Keeley SPE, Sutton RT, Shaffrey LC (2012) The impact of North Atlantic sea surface temperature errors on the simulation of North Atlantic European region climate. *Q J R Meteorol Soc* 138:1774–1783. doi:[10.1002/qj.1912](https://doi.org/10.1002/qj.1912)
- Knight JR et al (2005) A signature of persistent natural thermohaline circulation cycles in observed climate. *Geophys Res Lett* 32:L20708. doi:[10.1029/2005GL024233](https://doi.org/10.1029/2005GL024233)
- Latif M (2013) The oceans' role in modeling and predicting decadal climate variations. In: Siedler G, Griffies S, Gould J, Church J (eds) *Ocean circulation and climate, 2nd edn. A 21st century perspective. International Geophysics Series, Volume 103*, ISBN: 9780123918512. Academic Press, New York
- Latif M et al (2004) Reconstructing, monitoring, and predicting multidecadal-scale changes in the North Atlantic thermohaline circulation with sea surface temperature. *J Climate* 17:1605–1614
- Latif M et al (2006) Is the thermohaline circulation changing? *J Climate* 19:4631–4637
- Manabe S, Stouffer RJ (1988) Two stable equilibria of a coupled ocean–atmosphere model. *J. Climate* 1:841–866
- Marshall J, Schott F (1999) Open-ocean convection: observations, theory, and models. *Rev Geophys* 37(1):1–64. doi:[10.1029/98RG02739](https://doi.org/10.1029/98RG02739)
- Marshall J, Johnson H, Goodman J (2001) A study of the interaction of the North Atlantic oscillation with ocean circulation. *J Climate* 14:1399–1421
- Park W et al (2009) Tropical Pacific Climate and its response to global warming in the Kiel Climate Model. *J Climate* 22:71–92
- Rayner NA et al (2003) Global analyses of sea surface temperature, sea ice, and night marine air temperature since the late nineteenth century. *J Geophys Res* 108(D14):4407. doi:[10.1029/2002JD002670](https://doi.org/10.1029/2002JD002670)
- Sausen R, Barthel K, Hasselmann K (1988) Coupled ocean–atmosphere models with flux correction. *Clim Dyn* 2:145–163
- Scaife AA, Copestey D, Gordon C, Harris C, Hinton T, Keeley S, O'Neill A, Roberts M, Williams K (2011) Improved Atlantic winter blocking in a climate model. *Geophys Res Lett* 38:L23703. doi:[10.1029/2011GL049573](https://doi.org/10.1029/2011GL049573)
- Taylor KE, Stouffer RJ, Meehl GA (2012) An overview of CMIP5 and the experiment design. *Bull Am Meteorol Soc* 93:485–498. doi:[10.1175/BAMS-D-11-00094.1](https://doi.org/10.1175/BAMS-D-11-00094.1)
- Thompson DWJ, Wallace JM (1998) The Arctic oscillation signature in the wintertime geopotential height and temperature fields. *Geophys Res Lett* 25(9):1297–1300
- Tonboe R, Eastwood S, Lavergne T, Pedersen LT (2011) EUMETSAT OSI SAF global sea ice concentration reprocessing data. Nimbus-7 SMMR and DMSP SSM/I-SSMIS Passive Microwave Data. National Snow and Ice Data Center, Boulder
- Wang C, Zhang L (2013) Multidecadal ocean temperature and salinity variability in the Tropical North Atlantic: linking with the AMO, AMOC, and subtropical cell. *J Climate* 26:6137–6162
- Wang C et al (2014) A global perspective on CMIP5 climate model biases. *Nature Climate Change* 4:201–205. doi:[10.1038/nclimate2118](https://doi.org/10.1038/nclimate2118)
- Zhang R, Delworth TL (2006) Impact of Atlantic multidecadal oscillations on India/Sahel rainfall and Atlantic hurricanes. *Geophys Res Lett* 33:L17712. doi:[10.1029/2006GL026267](https://doi.org/10.1029/2006GL026267)